Published in "Cell Metabolism 15(3): 311–323, 2012"
which should be cited to refer to this work.

Klf15 Orchestrates Circadian Nitrogen Homeostasis

Darwin Jeyaraj,[1,4] Frank A.J.L. Scheer,[5,10] Jürgen A. Ripperger,[6,10] Saptarsi M. Haldar,[1] Yuan Lu,[1] Domenick A. Prosdocimo,[1] Sam J. Eapen,[1] Betty L. Eapen,[1] Yingjie Cui,[1] Ganapathi H. Mahabeleshwar,[1] Hyoung-gon Lee,[2] Mark A. Smith,[2] Gemma Casadesus,[3] Eric M. Mintz,[7] Haipeng Sun,[8] Yibin Wang,[8] Kathryn M. Ramsey,[9] Joseph Bass,[9] Steven A. Shea,[5] Urs Albrecht,[6] and Mukesh K. Jain[1,*]

[1]Case Cardiovascular Research Institute, Harrington Heart and Vascular Institute, Department of Medicine
[2]Department of Pathology
[3]Department of Neurosciences
[4]Heart and Vascular Research Center, MetroHealth Campus Case
Western Reserve University, Cleveland, OH 44106, USA
[5]Division of Sleep Medicine, Brigham and Women's Hospital and Harvard Medical School, Boston, MA 02115, USA
[6]Department of Medicine, Division of Biochemistry, University of Fribourg, 1700 Fribourg, Switzerland
[7]Department of Biological Sciences, Kent State University, Kent, OH 44242, USA
[8]Department of Anesthesia, UCLA, Los Angeles, CA 90095, USA
[9]Department of Medicine, Northwestern University Feinberg School of Medicine, Chicago, IL 60611, USA
[10]These authors contributed equally to this work.
*Correspondence: mukesh.jain2@case.edu

http://doc.rero.ch

SUMMARY

Diurnal variation in nitrogen homeostasis is observed across phylogeny. But whether these are endogenous rhythms, and if so, molecular mechanisms that link nitrogen homeostasis to the circadian clock remain unknown. Here, we provide evidence that a clock-dependent peripheral oscillator, Krüppel-like factor 15 transcriptionally coordinates rhythmic expression of multiple enzymes involved in mammalian nitrogen homeostasis. In particular, Krüppel-like factor 15-deficient mice exhibit no discernable amino acid rhythm, and the rhythmicity of ammonia to urea detoxification is impaired. Of the external cues, feeding plays a dominant role in modulating Krüppel-like factor 15 rhythm and nitrogen homeostasis. Further, when all behavioral, environmental and dietary cues were controlled in humans, nitrogen homeostasis exhibited an endogenous circadian rhythmicity. Thus, in mammals, nitrogen homeostasis exhibits circadian rhythmicity, and is orchestrated by Krüppel-like factor 15.

INTRODUCTION

Despite its abundance in the earth's atmosphere, mammals cannot freely assimilate nitrogen and are dependent on ingestion of amino acids (AAs). Nitrogen fixation is an elementary biological process through which microorganisms that exist in the roots of leguminous plants convert atmospheric nitrogen to ammonia. Thus, plants serve as the major source of AAs for mammalian organisms. Accordingly, AAs in organisms are termed essential (diet-dependent) or nonessential (synthesized from other essential AAs in vivo). In addition to serving as building blocks of proteins, AAs are critical for diverse biological functions, including gluconeogenesis, hormone synthesis, nutrient signaling, neurotransmission, and embryonic stem-cell growth (Wang et al., 2009; Wu, 2009). Following utilization of AAs, organisms also face the burden of detoxifying the by-products (i.e., converting ammonia to urea) (Morris, 2002). The importance of this homeostatic process is perhaps best demonstrated in congenital disorders of AA metabolism/ammonia detoxification that often present with dysfunction of multiple organ systems, particularly cognitive impairment (Gropman et al., 2007). Recent studies have also shed light on a potentially direct pathogenic role for AAs. Interestingly, supplementation of essential AAs significantly reduced survival in *Drosophila* (Grandison et al., 2009), whereas supplementation of branched chain AAs (BCAA) enhanced survival in mice (D'Antona et al., 2010). Thus, organisms face a delicate task of imbibing and metabolizing AAs, and imbalance alters survival.

The behavior, activity, and survival of organisms are influenced by the 24-hr rotation of the earth on its axis (Foster and Roenneberg, 2008). Studies over the last two decades have identified components of the endogenous core clock machinery (CCM) that govern 24-hr rhythms even in the absence of external cues (e.g., light) (Reppert and Weaver, 2002). The CCM exists in the central circadian pacemaker in the hypothalamus and the suprachiasmatic nucleus, as well as in most peripheral cells, and consists of a series of positive and negative feedback loops generated by the basic helix-loop-helix family of transcription factors *Clock* and *Bmal1*, the Period and Cryptochrome families, and the nuclear receptors *Reverbα* and *Rorα* (Ko and Takahashi, 2006). The CCM in the suprachiasmatic nucleus is entrained by cues, such as light exposure, and acts via neural and endrocrine signals to appropriately synchronize the CCM in peripheral tissues (Dibner et al., 2010). However, circadian timing in peripheral tissues many also be affected by other factors, such as rhythmic feeding and temperature (Dibner et al., 2010). Multiple lines of evidence identify the CCM as centrally involved in regulating metabolic homeostasis, particularly with respect to glucose and lipid levels (Duez and Staels, 2008; Green et al., 2008; Lamia et al., 2008; Le Martelot et al., 2009; Marcheva

et al., 2010; Rudic et al., 2004; Turek et al., 2005; Yin et al., 2007). A relationship of the CCM to AA utilization and excretion (i.e., nitrogen homeostasis) remains unknown.

Interestingly, several aspects of nitrogen flux across phylogeny occur in a diurnal fashion. The first process of nitrogen fixation in diazotrophs is highly diurnal due to the oscillatory pattern of nitrogenase activity (Balandreau et al., 1974; Wheeler, 1969). As a consequence, AA concentration in the leaves of plants exhibit diurnal variation (Bauer et al., 1977). Intriguingly, studies from humans and rodents more than five decades ago reported diurnal variation in plasma levels of AAs that is modulated by changes in diet (Feigin et al., 1967, 1969; Fernstrom et al., 1979). Further, recent unbiased metabolite analyses in yeast and mice determined that AAs and urea-cycle intermediates exhibit oscillatory behavior (Minami et al., 2009; Tu et al., 2007). In addition, screening of the hepatic proteome revealed rhythmicity of AA metabolic enzymes and urea cycle enzymes (Reddy et al., 2006). However, the molecular mechanisms that control these diurnal rhythms and determine whether nitrogen homeostasis exhibits true endogenous circadian rhythmicity (i.e., oscillation in the absence of external cues) remain unknown.

Krüppel-like factors belong to the zinc-finger family of transcription factors and are implicated in coordinating numerous biological processes from pluripotency to carcinogenesis (McConnell and Yang, 2010). Our laboratory previously demonstrated that Krüppel-like factor 15 *(Klf15)* regulates glucose homeostasis through effects on AA metabolism (Gray et al., 2007). Subsequent genome-wide microarray analyses of muscle and liver tissues identified additional targets of *Klf15* as being involved in AA metabolism. Thus, we hypothesized that *Klf15* may be involved in regulating the rhythmic utilization of AAs. In the present study we demonstrate that nitrogen homeostasis exhibits 24-hr periodicity in mice and humans. Further, we identify *Klf15* as a clock-dependent peripheral regulator of rhythmic AA utilization and excretion of AAs.

RESULTS

Klf15 Expression Exhibits 24-Hour Periodicity

As a first step, we examined whether *Klf15* expression itself was rhythmic. Wild-type (WT) mice were sacrificed every 4 hr under light/dark (L/D) or constant dark (D/D) conditions for 24 hr. *Klf15* expression exhibits rhythmic oscillation in several peripheral organs, including liver and skeletal muscle, under both conditions (Figures 1A, 1B, 1C, S1A, available on line, and S1B), confirming the notion that *Klf15* expression is rhythmic. As next steps, we examined whether the CCM mediates *Klf15* rhythmicity in peripheral organs and also, how this occurs. Examination of the regulatory region of *Klf15* identified four E-box binding motifs (Figure 1D, inset), and CLOCK/BMAL1 induced *Klf15* in a dose-dependent manner in hepatocyte cell lines (Figure 1D). Consistent with this observation, *Klf15* rhythmic variation was abrogated in *Bmal1* null livers (Figure 1E). Further, *Klf15* rhythmicity was also abrogated in livers of several CCM mutant mouse lines, including *Per2*/*Cry1* KO, *Per1*/*2* KO, and *Reverbα* KO (Figures S1C and S1D). Finally, chromatin immunoprecipitation (ChIP) revealed rhythmic occupancy of *Bmal1* on the *Klf15* promoter (Figure 1F). These data support a direct role for the CCM in orchestrating the 24-hr periodicity of *Klf15.*

Nitrogen Homeostasis Exhibits 24-Hour Periodicity in Mice

In addition to daily rhythms in *Klf15*, we next examined whether AA utilization and excretion also oscillate. WT mice were placed in constant darkness for 38 hr (D/D), after which plasma was collected every 4 hr for the following 24 hr. Interestingly, the total AA pool, as well as major circulatory AAs (e.g., alanine and BCAAs exhibited 24-hr rhythms in constant darkness) (Figures 2A, 2B, and 2C). Further, the detoxified excretory product of nitrogeneous waste (i.e., urea) also oscillates with similar 24-hr periodicity) (Figure 2D). Of the 20 AAs, 14 were rhythmic under D/D, as detailed in Table S1. Thus, nitrogen homeostasis in mice exists with a 24-hr periodicity even under constant environmental conditions.

Klf15 Regulates Rhythmic Amino Acid Utilization

Next, the effect of *Klf15* proficiency and deficiency on nitrogen homeostasis was assessed under L/D over a 24-hr period. Because mammals are dependent on diet for essential AAs, we first assessed the cumulative and total food intake over 24 hr. The cumulative food intake (measured every 5 min, Figure 2E) and aggregate food consumed over 24 hr (Figure S2A) were nearly identical in WT and *Klf15* null mice. Consistent with this observation, the total body weights of *Klf15* null mice were similar to their WT counterparts (Figure 2F). Further, the free running period under constant-dark and constant-light conditions were similar between WT and *Klf15* null mice (Figures S2B and S2C). Interestingly, the hepatic expression of oscillation of several components of the CCM was preserved in the *Klf15*-deficient state (Figure S2D). However, a marked alteration in both the absolute levels and rhythmicity of the total AA pool and urea were observed in *Klf15* null mice (Figures 3G and 3H). A detailed analysis of each individual AA is provided in Table S1. Collectively, these observations identify *Klf15* as an essential regulator of rhythmic nitrogen homeostasis.

We next sought to elucidate the molecular basis for the non-rhythmic nitrogen homeostasis in the *Klf15*-deficient state. In mammals, the liver and skeletal muscles are centrally involved in coordinating nitrogen homeostasis. During the daily feed/fast rhythms, the glucose-alanine cycle serves two main purposes: 1) supplying carbon skeletons to the liver to sustain glucose levels, and 2) facilitating transport and elimination of nitrogenous waste (Felig, 1975). During the fed state, when glucose is freely available, skeletal muscle oxidizes glucose to generate pyruvate, which is transaminated by alanine transaminase (*Alt*) to produce alanine (Figure 3 schematic) (Felig, 1975). Further, in the postabsorptive state, carbons generated from breakdown of muscle AAs are the principal precursors for hepatic gluconeogenesis. Because BCAA comprise 35% of the essential AAs in muscle (Harper et al., 1984), they are major donors of carbon and dispose their nitrogen through the glucose-alanine cycle. The skeletal muscle mitochondrial branched-chain transaminase (*Bcat2*) is the first step in BCAA catabolism and converts BCAA to glutamate and α-keto acids (Harper et al., 1984). The glutamate is subsequently utilized by *A*lt in skeletal muscle to synthesize alanine. The alanine spills

http://doc.rero.ch

http://doc.rero.ch

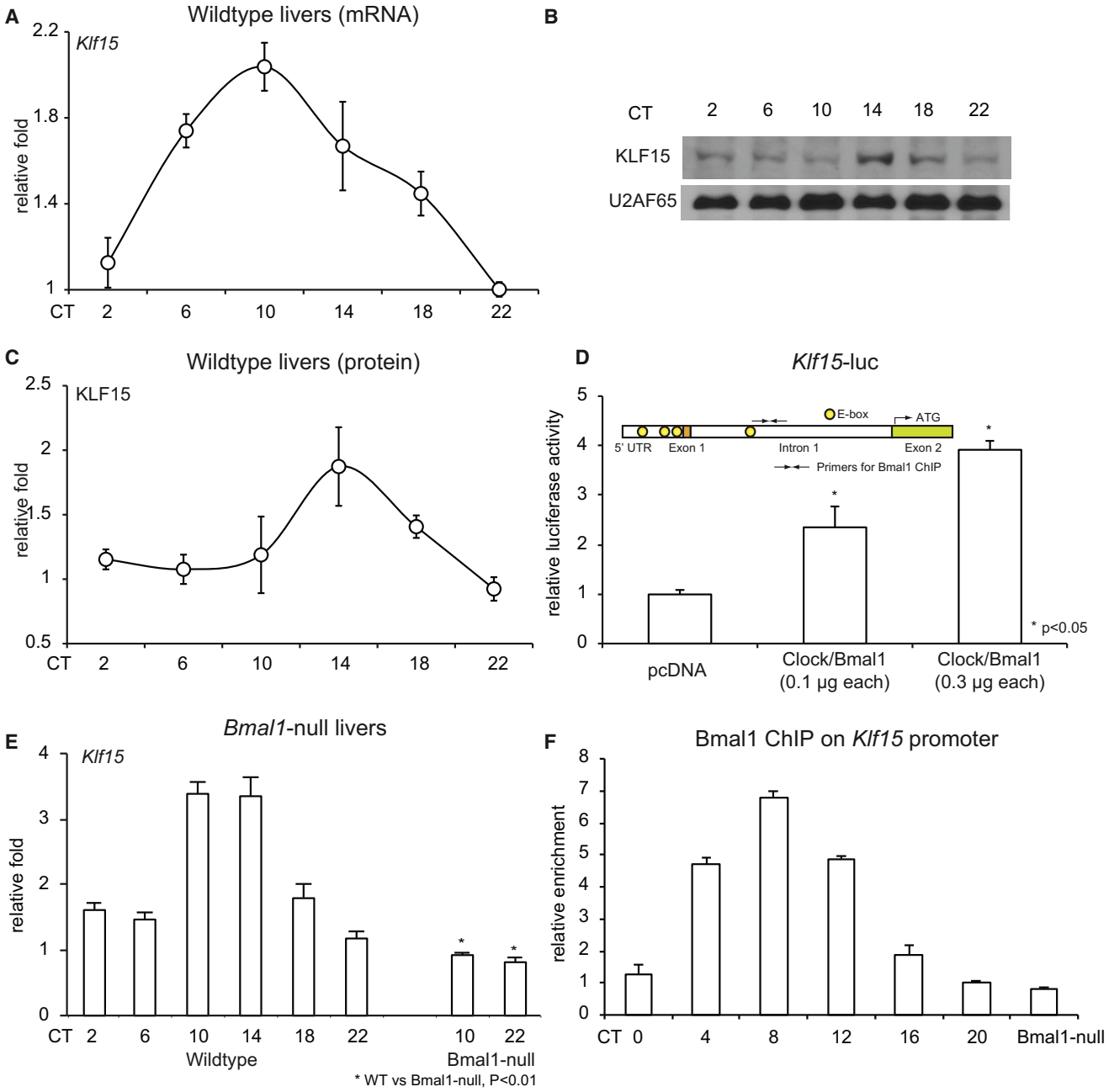

Figure 1. *Klf15* Exhibits 24-hr Periodicity and Is Driven by the Core Clock Machinery

(A) *Klf15* mRNA accumulation from WT mice livers (n = 5 per time point).

(B) Representative KLF15 and U2AF65 protein expression from WT and *Klf15* null liver nuclei.

(C) KLF15 protein densitometry from three replicates.

(D) *Klf15*-luciferase is induced in a dose-dependent fashion by CLOCK/BMAL1; inset illustrates four E-Box motifs in the *Klf15* promoter (−5 kb).

(E) *Klf15* mRNA accumulation in WT and *Bmal1* KO livers.

(F) Rhythmic binding of BMAL1 on the *Klf15* promoter (n = 3 per time point). Data presented as mean ± SEM.

into the circulation, is absorbed by the liver, and ultimately donates its carbons for gluconeogenesis and its nitrogen for urea synthesis (Figure 3 schematic). Intriguingly, the expression patterns of *Alt*, *Bcat2* in skeletal muscle and *Alt* in liver of WT mice were found to exhibit robust diurnal rhythms, an effect that was abrogated in both tissues with *Klf15*-deficiency (Figures 3A, 3B,and S3A). Consistent with this defect, skeletal muscle and liver concentrations of alanine and glutamate were reduced, and BCAA was significantly increased (Figure S3A). Consequently, plasma alanine was reduced without rhythmicity (Figure 3C), whereas plasma BCAA was persistently increased with abnormal rhythmicity in *Klf15* null mice (Figure 3D). An important

http://doc.rero.ch

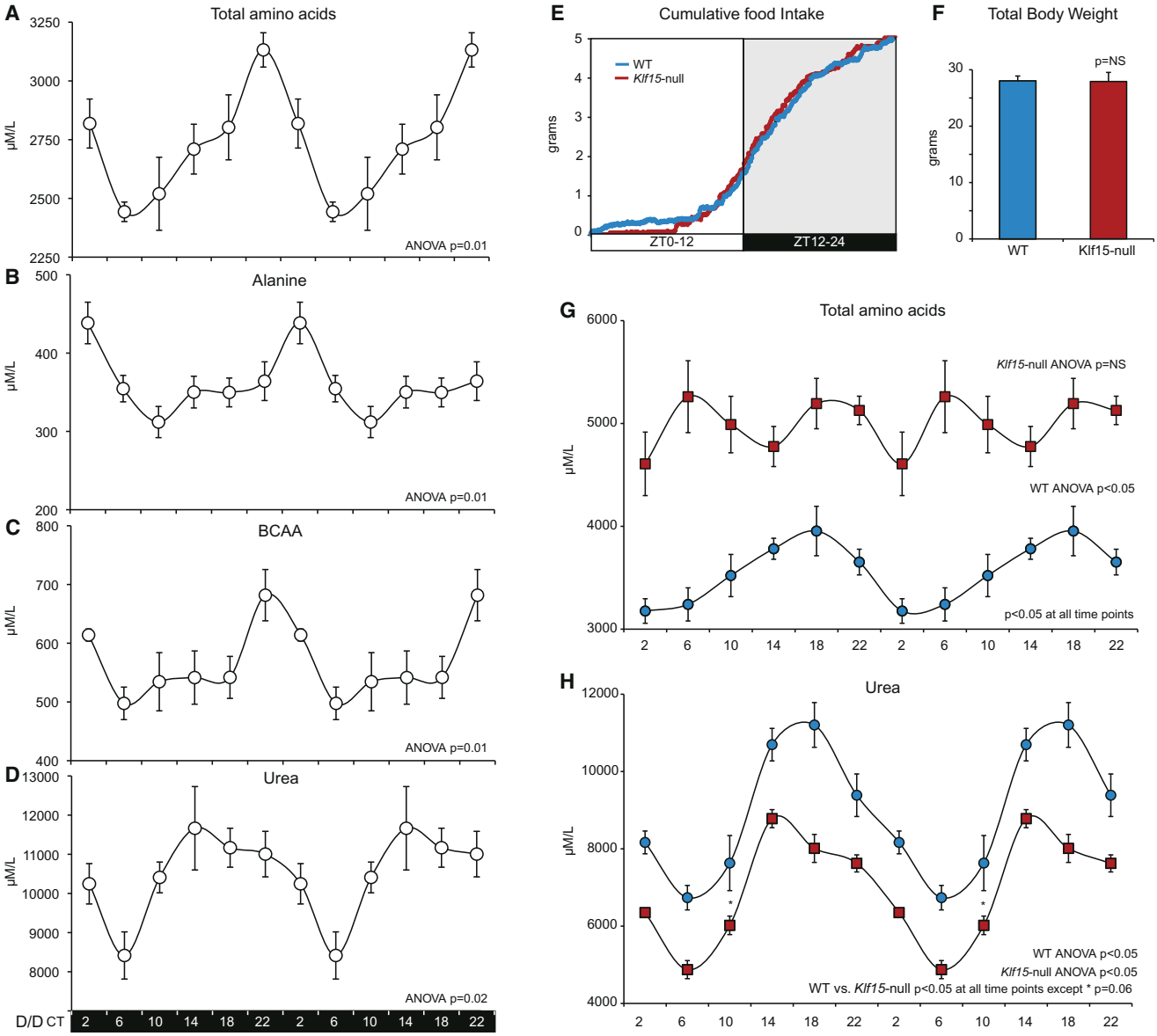

Figure 2. Nitrogen Homeostasis Exhibits 24-Hour Periodicity, Driven by *Klf15*, in Mice

(A–D) Plasma total AA pool, alanine, BCAA, and urea measured every four hours over a circadian period after placing mice in constant darkness for 38 hr (n = 5 per time point). The data are double-plotted, and ANOVA was used to determine rhythmicity.

(E) Cumulative food intake measured every 5 min in WT and *Klf15* null mice (n = 4 per group).

(F) Total body weights of WT and *Klf15* null mice (n = 4 per group).

(G and H) Plasma total AA pool, urea from WT and *Klf15* null mice measured every 4 hr under L/D and double-plotted to illustrate rhythmicity (n = 5 per group per time point). Data presented as mean ± SEM.

consequence of impaired alanine availability was persistently low glucose in *Klf15* null mice (Figure 3E). This occurred despite compensatory adaptive changes in several hepatic gluconeogenic enzymes (*Glut2*, *Pepck*, *Pfkfbp2*, *and G6PC*, Figure S3B), insulin, and glucagon (Figure S3B). Next, to examine whether *Alt* and *Bcat2* were direct transcriptional targets for *Klf15*, we utilized gain-of-function studies and ChIP. Adenoviral overexpression of *Klf15* induced *Alt* in hepatocytes and *Alt*, *Bcat2* in skeletal myotubes (Figure S3C). Further, AA analysis of cell-culture supernatant from *Klf15* overexpressing hepatocytes revealed reduced alanine and increased glutamate concentrations (Figure S3C). Examination of the *Alt* promoter region identified conserved consensus DNA-binding sites for Krüppel-like factors C(A/T)CCC (Miller and Bieker, 1993) (Figure S3D). Finally, ChIP analysis of WT livers over a circadian period identified rhythmic enrichment of KLF15 on the *Alt* promoter (Figures 3f and S3D).

Klf15 Regulates Rhythmic Urea Synthesis

The final common pathway in liver for detoxification of nitrogenous waste occurs through glutamate, the major nitrogen donor

http://doc.rero.ch

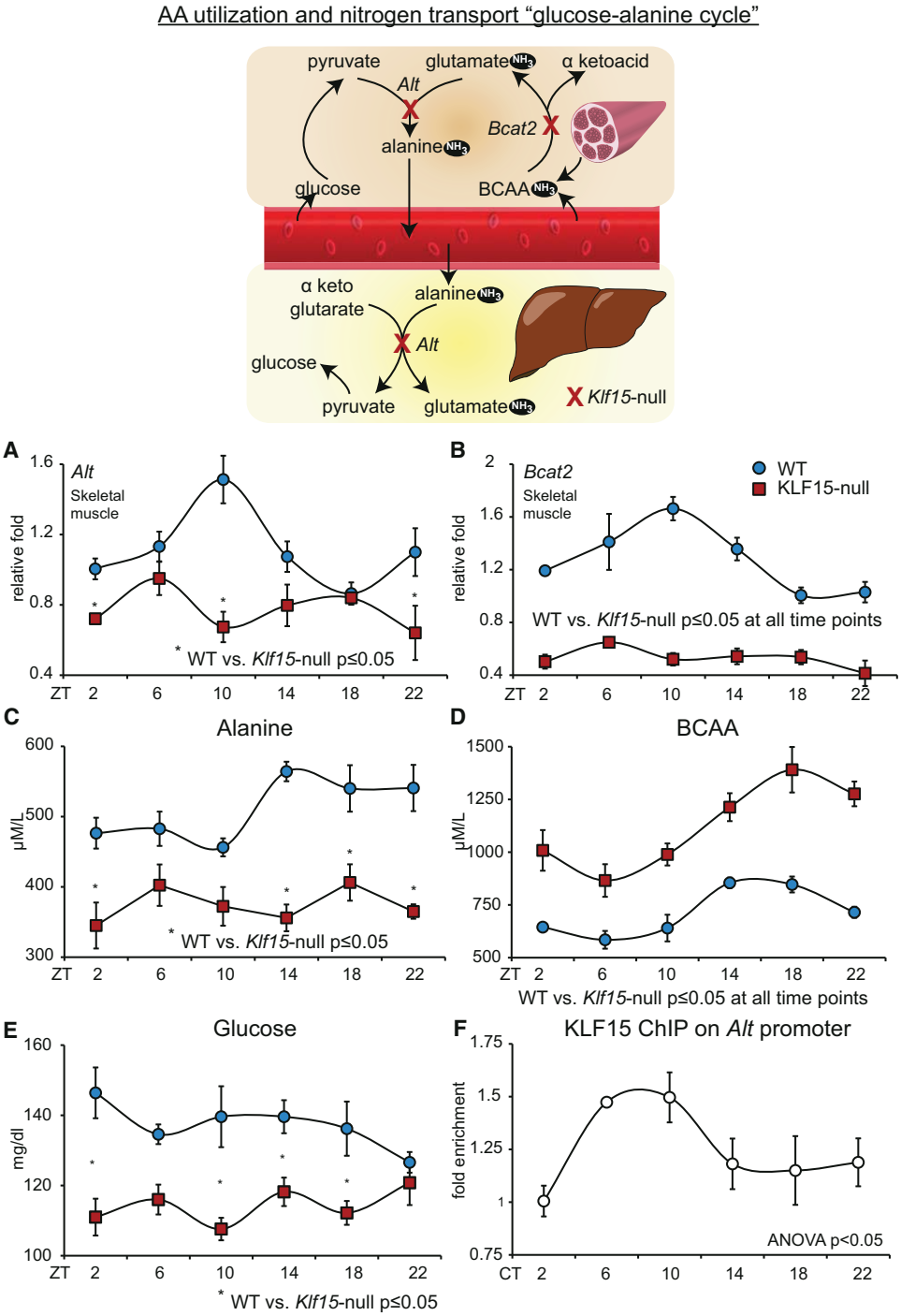

Figure 3. *Klf15* Regulates Rhythmic Amino Acid Utilization

Schematic illustrates the interorgan transport and utilization of AAs (i.e., the glucose-alanine cycle).

(A and B) Skeletal muscle *Alt* and *Bcat2* expression in WT and *KLF15* null mice (n = 4 per group per time point).

(C and D) Plasma alanine and BCAA in WT and *Klf15* null mice (n = 5 per group per time point).

(E) Plasma glucose in WT and *Klf15* null mice (n = 5 per group per time point).

(F) ChIP for KLF15 on *Alt* promoter (n = 3 per time point). (# $p < 0.05$ at all time points between WT and *Klf15* null). Data presented as mean ± SEM.

for ammonia (Brosnan and Brosnan, 2009). Surprisingly, despite reduced plasma glutamate in *Klf15* null mice (Figure 4A), the plasma ammonia levels were increased (Figure 4B). This led us to examine expression of the hepatic urea-cycle enzymes. The urea cycle (Figure 4 schematic) is responsible for detoxification of ammonia to urea and occurs predominantly in the

http://doc.rero.ch

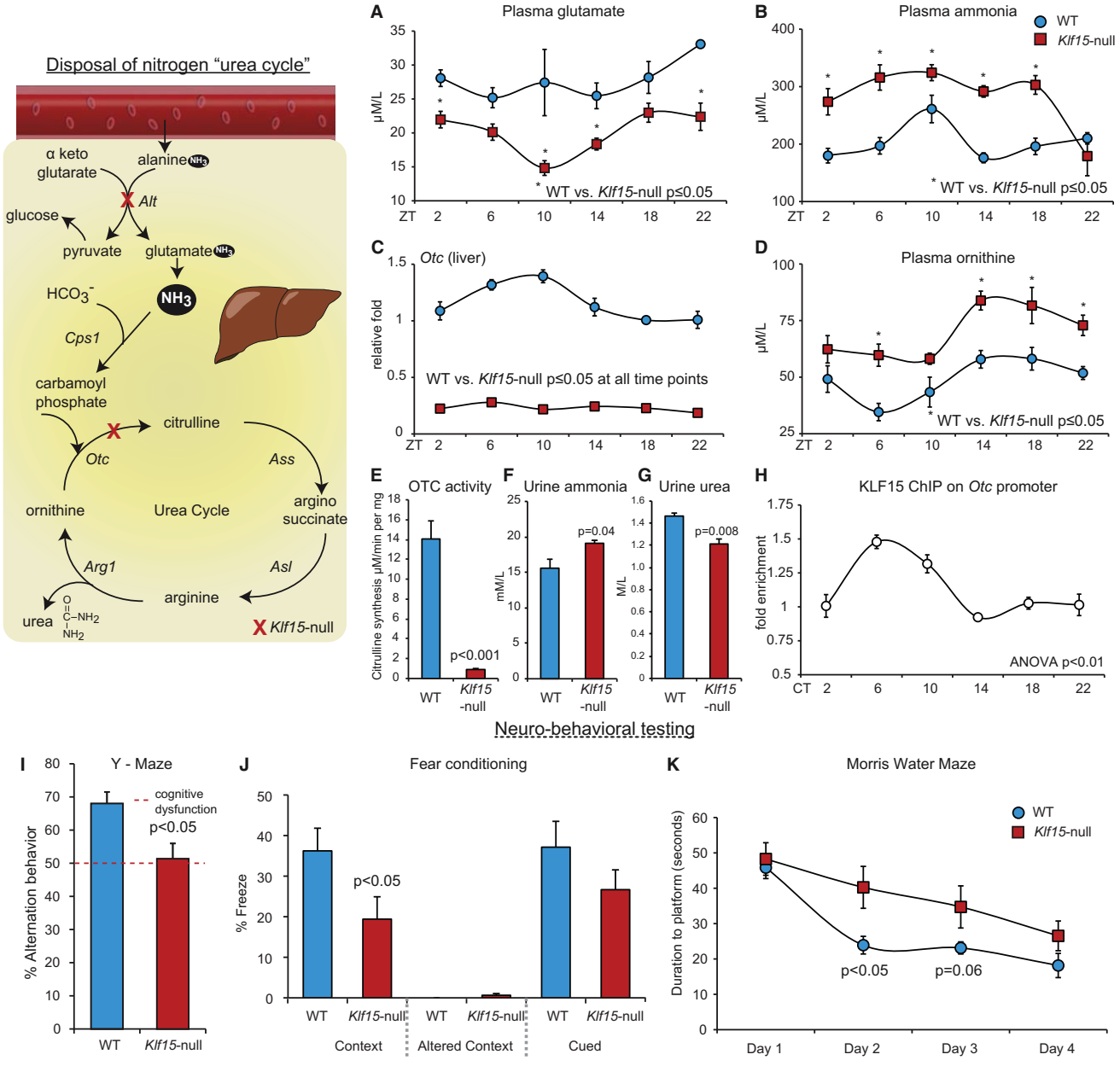

Figure 4. *Klf15* Regulates Rhythmic Nitrogeneous Waste Excretion

Schematic illustrates the excretion of nitrogenous waste products (i.e., the urea cycle).

(A and B) Plasma glutamate, ammonia in WT and *Klf15* null mice (n = 5 per group per time point).

(C) *Otc* expression in WT and *Klf15* null livers (n = 4 per group per time point).

(D) Plasma ornithine in WT and *Klf15* null mice (n = 5 per group per time point).

(E) OTC enzymatic activity measured from liver mitochondrial extracts from WT and *KLF15* null mice (n = 4 per group).

(F and G) Urinary levels of urea and ammonia in WT and *KLF15* null mice (n = 5 per group).

(H) ChIP for KLF15 on the *Otc* promoter (n = 3 per time point). (# p < 0.05 at all time points between WT and *Klf15* null).

(I–K)Results of neurobehavioral testing for (i) Y-maze, a test of working memory (n = 3 per group).

(J and K) Fear conditioning during contextual changes (hippocampal function) and altered cues (amygdalar function) (n = 8 per group) (J), and Morris water maze test, a test of hippocampal function (n = 8 per group) (K). Data presented as mean ±SEM.

mammalian liver (Morris, 2002). Interestingly, the expression of ornithine transcarbamylase (*Otc*), a hepatic mitochondrial urea-cycle enzyme was markedly reduced and devoid of rhythmicity in *Klf15* null mice (Figure 4C). In contrast, the 24-hr periodicity of expression of other urea-cycle enzymes (*Cps1*, *Asl*, *Ass*, *and Arg1*) was either unchanged or increased with *Klf15* deficiency (Figure S4A). Importantly, OTC enzymatic activity from KLF15 null hepatic mitochondrial extracts was reduced to ~ 6% of their WT counterparts (Figure 4E). Consistent with this defect, plasma/tissue concentrations of ornithine were markedly

increased (Figures 4D and S4B). Further, urine analysis revealed elevated levels of ammonia and reduced urea, supportive of impaired hepatic ureagenesis (Figures 4F and 4G). Next, to examine whether *Otc* is a transcriptional target for *Klf15*, we performed adenoviral overexpression in hepatocytes and ChIP. *Klf15* overexpression induced *Otc* expression, and analysis of hepatocyte cell culture supernatant revealed reduced ornithine concentration (Figure S4C). Further, ChIP identified rhythmic enrichment of KLF15 on a conserved region of the *Otc* promoter (Figures 4H and S4C). Next, to determine whether the observed hyperammonemia was associated with cognitive dysfunction, we performed extensive neurocognitive behavioral testing. *Klf15* null mice exhibited significant dysfunction of short-term memory, as evidenced by reduced percentage of alternation behavior in the Y-maze test (Figure 4I). To test for memory more specifically, we determined contextual (hippocampal) and cued (amygdala) fear-based memory. *Klf15* null mice exhibit reduced freezing in the context in which they had previously received an aversive stimulus suggestive of impaired hippocampal-based memory (Figure 4J). However, no significant difference was noted for cued fear conditioning (Figure 4J). Finally, in the Morris water maze, a selective test for hippocampal function, *Klf15* null mice exhibit an initial significant impairment in learning but no differences in retention, suggesting that *Klf15* null mice exhibit delay in learning but ability to ultimately acquire and retain the task (Figure 4K). In summary, these data suggest that impaired detoxification of ammonia impairs selective aspects of cognitive function in *Klf15* null mice.

Feeding Regulates Nitrogen Homeostasis and the Peripheral Core Clock Machinery

Previous studies determined that rhythmic feeding is a dominant input that modulates CCM expression in peripheral organs (Damiola et al., 2000). Thus, we reasoned that rhythmic feeding could alter *Klf15* diurnal expression pattern and nitrogen homeostasis. To test this hypothesis, mice were fed for a 6-hour period during the light phase (ZT3-ZT9) or ad libitum for a period of 1 month under L/D conditions. Animals were then harvested at two time points corresponding to the zenith and nadir of the total AA pool under L/D (Figure 2G). Consistent with previous studies (Damiola et al., 2000), restricting food intake to the light phase altered expression of several components of the CCM in liver, including *Clock*, *Per2*, *Cry1*, *Reverb*α, and *Dbp* (Figures 5A, 5B, 5C, and S5A). Interestingly, restricted feeding also altered expression of *Klf15* in liver and skeletal muscle, the total AA pool (including alanine and BCAA), ammonia, and urea (Figures 5D, 5E, 5F, 5G, and 5H). Of the 15 AAs that exhibit rhythmic oscillation in LD, the zenith and nadir of 13 were shifted significantly by daytime feeding (Table S1). Further, examination of enzymes in AA metabolism revealed alteration of *Alt* and *Bcat2* in skeletal muscle but not in the liver (Figures 5I, 5J, and S5B). Of the nitrogen-disposal machinery in the liver, *Otc* expression was reversed, and corroborated by changes in plasma ornithine (Figures 5K, 5L, and S5B). In an additional set of experiments, mice were harvested at all time points of a 24-hr period following restricted feeding. Consistent with our aforementioned experiments, we identified a full reversal in gene expression of *Bmal1*, *Klf15*, *and Otc* in the liver (Figure S5C). Thus, feeding rhythms play a key role in modulating *Klf15* and rhythmic nitrogen homeostasis.

Adaptation to High-Protein Diet in Wild-Type and *Klf15* Null Mice

Our study suggests an important role for *Klf15* in regulating rhythmic flow of nitrogen by orchestrating rhythmic variation in expression of AA utilization and excretion enzymes across multiple organs. To further substantiate the importance of these regulatory effects in vivo, we challenged WT and *Klf15* null mice to a high-protein diet (70% protein as casein) or normal diet (18% protein) for 1 week. In WT mice, despite the low levels of carbohydrate in the high-protein diet (18.7% compared to 62.3% carbohydrate in normal diet), the mice were able to maintain euglycemia (Figure 6A) by extracting carbon skeletons from AAs (i.e., gluconeogenesis through greater *Klf15* and *Alt* expression) (Figures 6B and 6C). In addition, ammonia levels were also maintained at physiological levels by increasing ureagenesis (Figures 6E and 6F) accompanied by a significant increase in hepatic *Otc* expression (Figure 6D). In sharp contrast, *Klf15* null mice exhibit near-fatal hypoglycemia on high-protein diet (1 of 5 mice died at 1 week of high-protein diet due to severe hypoglycemia), and demonstrated significant accumulation of AAs in plasma, indicating impaired utilization of AAs (Figures 6A, 6B, and 6C). In addition, and consistent with a significant defect in hepatic *Otc* function (Figure 6D), *Klf15* null mice exhibited marked hyperammonemia with impaired ureagenesis (Figures 6E and 6F). This global failure of nitrogen flux and inability to adapt to high-protein diet further illustrates the role of *Klf15* in controlling utilization and excretion of nitrogen in mammalian organisms.

Nitrogen Homeostasis Is Circadian in Humans

Studies from the 1960s, conducted for 6 continuous days, clearly established that AAs exhibit diurnal rhythm in humans (Feigin et al., 1967). Our studies in mice suggested that such rhythms could occur in the absence of external cues. However, because food intake exhibits endogenous circadian rhythmicity in mice, we cannot determine whether nitrogen homeostasis is driven simply by the feeding/fasting cycle or by an endogenous circadian rhythm that is independent of dietary cues. Thus, to determine whether the circadian system per se influences nitrogen homeostasis in humans independent of environmental, behavioral and dietary influences, we scheduled individuals to live on 28-hr "days" for 7 cycles across 196 hr in persistent dim light as previously described (Scheer et al., 2009). This forced desynchrony protocol dissociates the behavioral sleep/wake and fasting/feeding cycle (imposed 28-hr cycle) from the circadian system (endogenous $\sim$ 24-hr cycle), thus allowing the determination of circadian-system influences not confounded by the influence of changes in behavior (including food intake) and environment (including light). In this way, blood samples were obtained in the fasted state ($\sim$12 hr after the last meal) at different internal circadian phases. Using this gold-standard method in human circadian research, we discovered that several AAs, including alanine and BCAA, exhibit robust endogenous circadian rhythms (Figures 7B and 7C). Of the 20 AAs, 6 exhibited endogenous circadian rhythmicity in humans (Figures 7 and S6), and the total AA pool demonstrated a trend toward

http://doc.rero.ch

http://doc.rero.ch

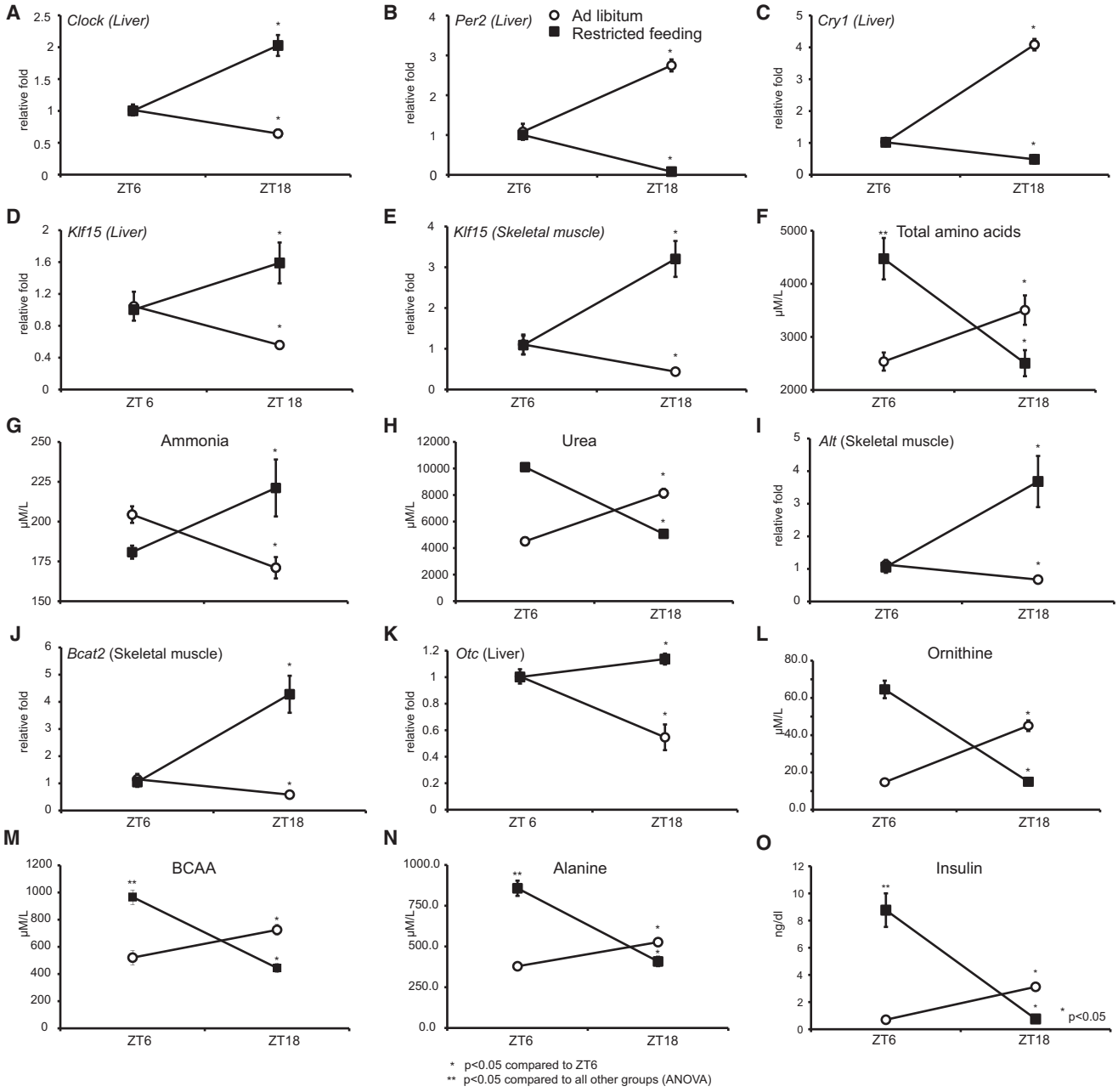

Figure 5. Feeding Alters *Klf15* Expression and Nitrogen Homeostatsis

(A–O) Following ad libitum feeding or feeding restricted to the light-phase (ZT3-ZT9) for one month: liver expression of *Clock*, *Per2*, and *Cry1* (A–C); liver and skeletal muscle expression of *Klf15* (D and E); total plasma AA, ammonia, and urea concentrations (F, G and H); skeletal muscle *Alt* and *Bcat2* expression (I and J); liver expression of *Otc* (K); and plasma ornithine, alanine, BCAA, and insulin (L, M, N, and O) (n = 5 per group per time point). Data presented as mean ± SEM.

rhythmicity (Figure 7A). Finally, plasma urea and ornithine also oscillated with endogenous ~ 24-hr periodicity (Figures 7D and S6).

DISCUSSION

Using complementary approaches in mice and humans, we demonstrate that nitrogen homeostasis is a conserved endogenous circadian process in mammals. Our initial studies in mice were done under the classical conditions to ascertain rhythmicity (i.e., constant darkness). In D/D we observed that 24-hr rhythmicity existed for total AA pool, ammonia, and urea (Figures 2A, 2B, 2C, and 2D). Furthermore, in our human study, we dissociated the influence of the circadian timing system from that of all environmental, behavioral, and dietary influences on nitrogen homeostasis by placing humans in persistent dim light for

http://doc.rero.ch

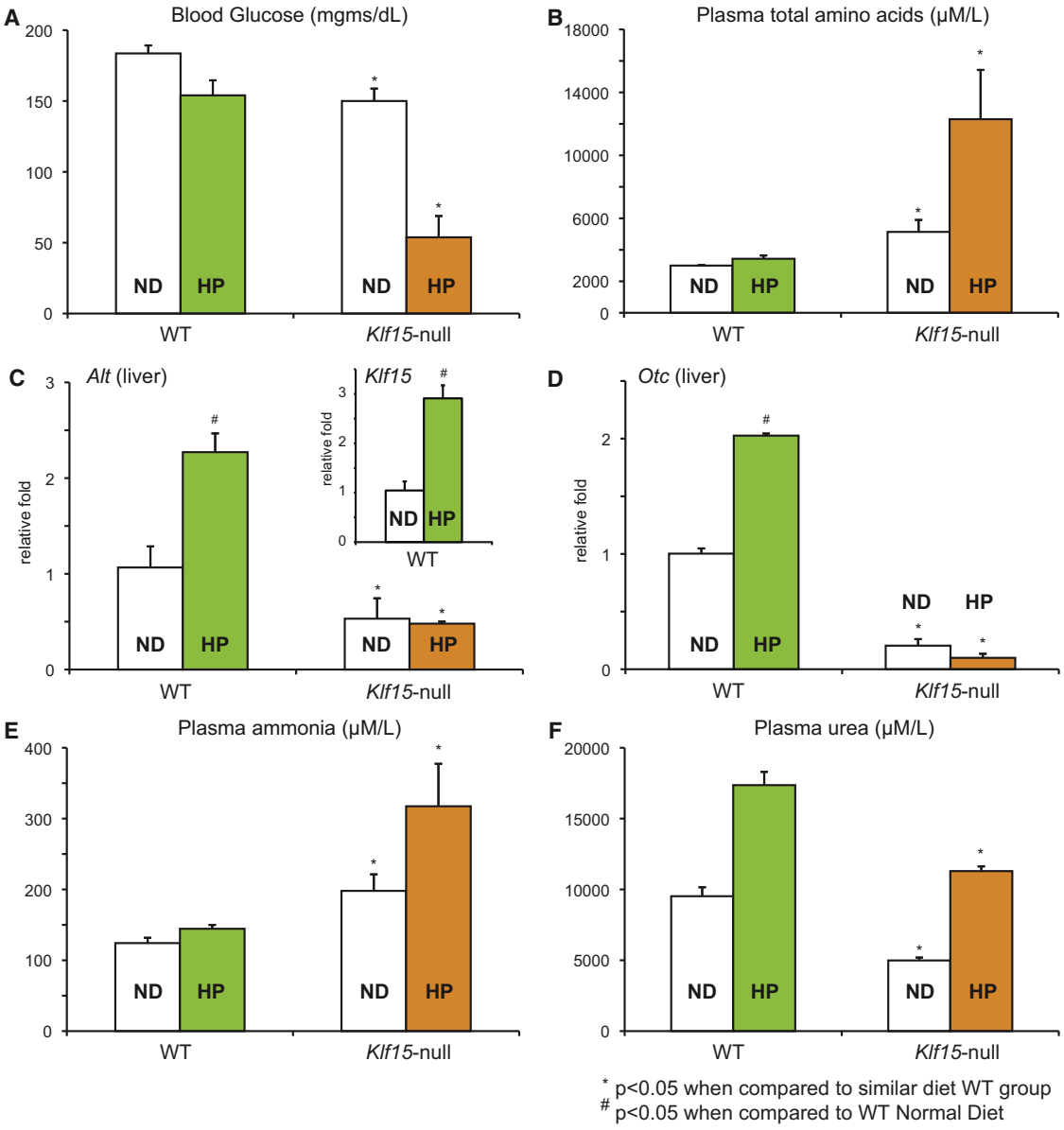

Figure 6. Wild-Type and *Klf15* Null Adaptation to High-Protein Diet

(A–E) Following 1 week of high-protein diet (HP; 70% casein) or normal diet (ND; 18% protein) WT and *Klf15* null (n = 5 per group) blood glucose (A), plasma AAs (B), liver expression of *Klf15*, *Alt*, and Otc (C and D), plasma ammonia (D), and plasma urea (E). Data presented as mean ± SEM.

196 hr and altering the habitual feed/fasting and sleeping rhythms to 28-hr cycles. Despite these alterations, nitrogen homeostasis proceeded with a 24-hr rhythmicity (Figure 7), which is convincing of an endogenous circadian driving force behind these rhythms.

The teleological role of circadian rhythms is postulated to coordinate behavioral rhythms (activity, feeding, sleeping) to the anticipated energetic needs of an organism (Green et al., 2008). Of these functions, glucose homeostasis is paramount due to the obligate use of glucose by the brain and limited ability of the mammalian liver to store glycogen. Therefore, within a few hours after a meal, AAs derived from skeletal muscle provide the carbon skeleton for hepatic gluconeogenesis (Felig, 1975). However, as a consequence of utilizing carbons from AAs, mammalian organisms face the burden of eliminating the toxic nitrogenous waste. Our study identifies *Klf15* as a clock-driven, peripheral circadian factor essential for coordinating delivery of the carbon skeletons required for glucose production and elimination of ammonia to urea. The importance of this regulation is underscored by the fact that failure to faithfully coordinate rhythmic utilization and excretion of AAs can lead to severe pathophysiological consequences. Indeed, failure of rhythmic AA utilization leads to persistently low glucose with impaired circadian glucose homeostasis (Figure 3), whereas failure of rhythmic excretion causes hyperammonemia and attendant cognitive dysfunction (Figure 4).

http://doc.rero.ch

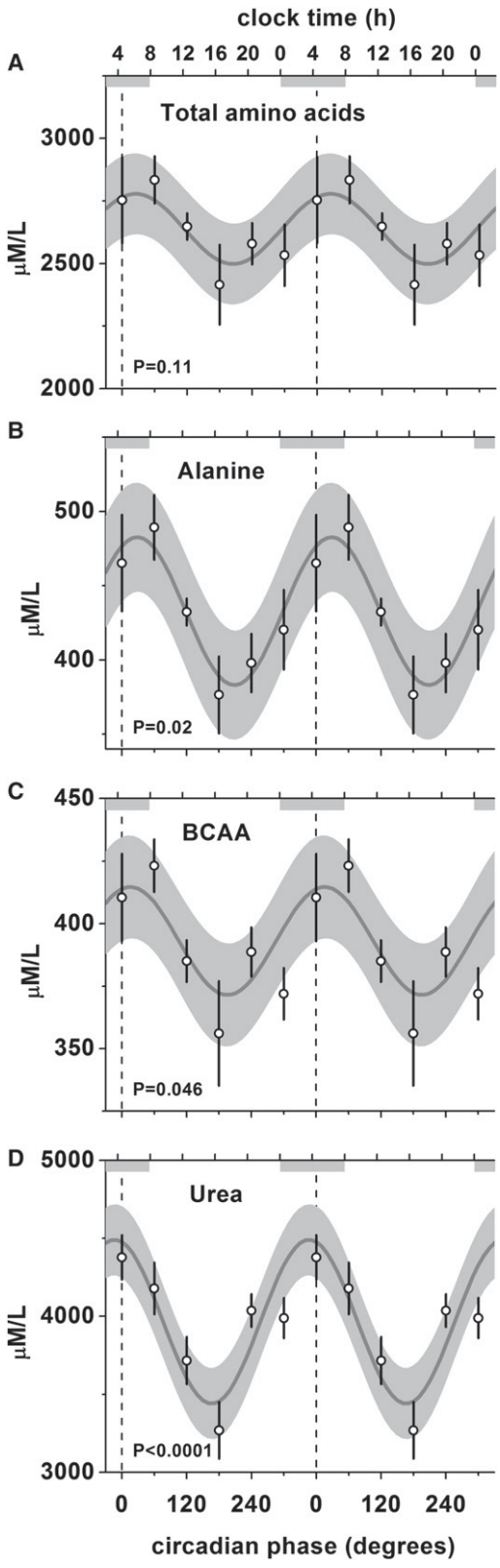

Figure 7. Human Endogeneous Circadian Nitrogen Homeostasis

Fasting total plasma AA pool, alanine, BCAA, and urea exhibit endogenous circadian rhythmicity in humans during the forced desynchrony protocol. The cosine models (black lines) and 95% confidence intervals (gray areas) are based on mixed-model analyses and use precise circadian phase data. To show that these models adequately fit the actual data, we also plot the proportional changes across 60 circadian degree windows per individual, multiplied by the group average with SEM error bars (open circles with error bars). Data are double-plotted to aid visualization of rhythmicity. Lower x axis shows the circadian phase in degrees, with fitted core body temperature minimum assigned 0° and 360° equal to the individual circadian period (group average = 24.09 hr); top x axis shows corresponding average clock time for these individuals; vertical dotted lines show core body temperature minimum; horizontal gray bars show corresponding average habitual-sleep episode in the 2 weeks prior to admission.

Our study also links the circadian clock to nitrogen homeostasis through a *Klf15*-dependent mechanism (see Graphical Abstract). *Klf15* rhythm was disrupted in several circadian clock-mutant mouse lines, and our data supports a direct clock-dependent transcriptional basis for this regulation (Figures 1E, S1C, and S1D). This was also confirmed in an independent genome-wide ChIP-sequencing study that identified rhythmic BMAL1 binding to the *Klf15* promoter (Rey et al., 2011). Feeding rhythms have been identified to play an important role in entraining the peripheral clock (Damiola et al., 2000). Further, depleting food intake led to failure of rhythmic variation of transcripts in the liver, whereas, restricted feeding in a Clock mutant-induced oscillation of several transcripts in the liver (Vollmers et al., 2009). Because nitrogen utilization and disposal largely occurs in peripheral organs, we examined the role of restricted feeding and identified that feeding plays an important role in rhythmic nitrogen homeostasis by altering expression of *Klf15* and other AA utilization enzymes (Figure 5). The essential role of *Klf15* in mediating AA rhythms was also evident from the observation that normal feeding/activity rhythms and near-normal hepatic clock gene expression rhythms (Figures 2 and S2) in Klf15 null mice were not sufficient to maintain AA rhythms. Further, administration of high-protein diet was not sufficient to overcome the enzymatic deficiencies caused by the absence of *Klf15* (Figure 6). Thus, our studies suggest a central role for *Klf15* in transcriptionally coupling rhythmic variation in AA metabolic enzymes to the circadian clock and feeding rhythms. There are several important limitations to our work. First, because *Klf15* is controlled by *Bmal1* (Figure 1), our observations suggest that the circadian clock may also control nitrogen homeostasis. However, studies assessing nitrogen homeostasis in Clock mutant or *Bmal1* null mice are likely to be confounded by abnormal feeding rhythms, altered food intake, and body composition (Turek et al., 2005; Shi et al., 2010). Further, because nitrogen homeostasis occurs across multiple organs, compound tissue-specific deletion models in Clock mutants will be needed to investigate this issue. Although such studies are decidedly nontrivial, they are clearly of interest and will provide a more comprehensive understanding of the link between the circadian clock and rhythmic nitrogen homeostasis in mammalian organisms.

Finally, because AAs can activate many signaling pathways and are precursors for hormones/nitrogenous substances (Wu, 2009), dysregulation of rhythmic utilization and excretion may play a pathogenic role in the onset of common disease states. For example, restricted feeding also resulted in a marked elevation of the total AA pool, BCAA, and alanine (Figures 5F, 5M, and 5N. Interestingly, this was associated with a significant increase

in plasma insulin (Figures 5O and S7). It is also consistent with the well-known relationship between shift work and insulin resistance (Scheer et al., 2009). Indeed, studies have identified a pathogenic role for altered BCAA levels in the development of insulin resistance (Newgard et al., 2009). More recently, Shah et al. identified a significant relationship between BCAA levels and urea-cycle metabolites in patients with coronary artery disease (Shah et al., 2010). Finally, *Klf15* null mice develop cardiac and vascular myopathy, characterized by heart failure and aneurismal aortic dilatation, following exposure to angiotensin II infusion (Haldar et al., 2010). These findings support a potential link between impaired nitrogen homeostasis and susceptibility to common disease states. Thus, examination of rhythmic changes in nitrogen homeostasis may have wide clinical implications for diagnosis, prognosis, and therapy.

EXPERIMENTAL PROCEDURES

Mice and Dietary Perturbations

All animal studies were performed in accordance with guidelines from the Institutional Animal Care Use Committee (IACUC) at Case Western Reserve University, Cleveland, OH, and at collaborating facilities. WT male mice on C57BL6/J background were purchased from The Jackson Laboratory (Bar Harbor, ME), and acclimatized to our facility for 3–4 weeks. Generation of systemic *Klf15* null mice was previously described (Fisch et al., 2007), and *Klf15* null mice have been backcrossed into the C57BL6/J background for over 10 generations. WT and *Klf15* null mice were housed under strict light/dark conditions (6:00 a.m. lights on and 6:00 p.m. lights off), and had free access to standard chow/water. For L/D experiments, mice were euthanized with $C0_2$ inhalation or isoflurane every 4 hr for 24 hr. For D/D experiments, mice were placed in complete darkness for 38 hr (starting at the end of light phase ZT12), followed by harvest every 4 hr over a 24-hr period. Studies on the Bmal1 null, *Per1/2* double-KO, *Per2/Cry1* KO, and *Reverba* were as previously described (Hogenesch et al., 2000; Oster et al., 2002; Preitner et al., 2002; Zheng et al., 2001). For restricted feeding studies, mice had free access to food (ad libitum group) or access only during the light phase ZT3-ZT9 for 1 month. High-protein diet feeding was conducted for 1 week. The control diet for this study consisted of 18.1% protein, 62.3% carbohydrate, and 6.2% fat (TD110483, Harlan Laboratories), and high-protein diet was 70% casein, 18.7% carbohydrate, and 6.2% fat (TD 03367, Harlan Laboratories).

Physiological Studies

Wheel-running behavior was monitored in mice using Clocklab software (Actimetrics). Animals were housed in L/D until stably entrained, then wheel running was recorded for 3 weeks in L/D, 3 weeks in D/D, and 17 days in L/L. Food intake analysis was measured using the DietMax system (Accuscan Instruments, Columbus, OH) every 5 min at the Cincinnati Mouse Metabolic Phenotyping core (MMPC).

Tissue Harvest and Biochemical Analysis

Prior to euthanasia, glucose was measured from tail blood using glucometer (Accu-Check, Roche Diagnostics). Following this, mice were euthanized and blood was collected from the inferior vena cava with a heparin-coated syringe. For constant-dark experiments, the optic nerves were severed following euthanasia and before proceeding to organ harvest. Organs were washed in cold phosphate-buffered saline and flash-frozen in liquid nitrogen. Plasma was separated by centrifugation and frozen in aliquots for analysis. Plasma insulin and glucagon were measured using radio-immuno assay, and AAs, ammonia, urea, and ornithine were measured using high-performance liquid chromatography at the Vanderbilt MMPC. Tissue AAs, ammonia, urea, and ornithine were extracted by homogenizing weighed tissue pieces in 10% 5-sulphosalicylic acid dissolved in distilled water. Briefly, AA analysis was performed using a Biochrom 30 analyzer, a PC-controlled automatic liquid chromatograph with a post-column detection system. Prepared samples are injected into a column of cation exchange resin and separated by buffers of varying pH and ionic strength. They are then reacted with ninhydrin at 1,350°C and the absorbance maxima is read at 440 and 570 nm. The retention time of the peak identifies the AA, and the area under the peak indicates the quantity present. Samples were prepared by deproteinizing with 10% SSA (5-sulfosalicylic acid) and centrifugation. The resulting supernatant was then added to an equal quantity of Lithium citrate loading buffer, which lowers the pH prior to introduction to the cation exchange column. A known quantity of Norleucine may also be added to act as an internal standard. The PC presents both a detailed chromatogram of each sample and the amount of each AA, based on comparison to a standard mixture of acidic and basic AAs. These results were confirmed by manual calculations based on the area of each peak.

OTC Activity Analysis

Hepatic mitochondrial extracts were prepared, and OTC activity measured as previously described (Lee and Nussbaum, 1989; Ye et al., 1996).

Cell Culture Studies

For adenoviral overexpression studies, Hepa1-6 cells or AML12 mouse hepatocyte cell lines and differentiated C2C12 cells were used. For AA analysis, adenoviral overexpression was performed for 48 hr in serum-free media. The media was removed, spun to remove debris, deproteinized, and analyzed for AA, ornithine concentration. The promoter region of *Klf15* (−5 kb before the translation start site in the second exon) was cloned into PGL3 reporter vector (Promega, Madison, WI). Transient transfection studies were conducted in HepG2 cells using Fugene HD (Roche, Indianapolis, IN).

RNA Isolation and Real-Time PCR Analysis

RNA was isolated from frozen liver and skeletal muscle samples by homogenization in Trizol reagent by following manufacturer's instructions (Invitrogen, Carlsbad, CA). RNA was reverse transcribed following DNase treatment. Real-time PCR was performed using standard or LNA-based Taqman approach with primers/probes designed and validated from the Universal Probe Library (Roche, Indianapolis, IN). The results were normalized to Beta actin or Gapdh.

Western Immunoblotting

Liver samples were homogenized in buffer containing 50 mM Tris, 150 mM NaCl, 1 mM EDTA, 1% Triton X-100, 0.5% sodium deoxycholate, and 1% SDS supplemented with protease and phosphatase inhibitors (Roche, Indianapolis, IN). Nuclear lysates were prepared using the NE-PER kit following manufacturer's instructions (Thermo Scientific, Rockford, IL). A goat polyclonal antibody against KLF15 was used (ab2647, Abcam, Cambridge, MA).

Chromatin Immunoprecipitation

Chromatin immunoprecipitation was performed from mouse livers as previously described (Tuteja et al., 2009; Ripperger and Schibler, 2006). Briefly, WT mouse livers were harvested every 4 hours and fixed with 1.1% formaldehyde for 10 min. Following this, chromatin was prepared and sonicated using Bioruptor (Diagnode, Sparta, NJ). The sonicated chromatin was flash frozen in liquid nitrogen and stored at −80°F for subsequent analysis. Immunoprecipitation was conducted using Dynabeads (Invitrogen, Carlsbad, CA) bound to BMAL1 or KLF15 antibody. The promoter regions of putative KLF15 target genes were manually examined for conserved regions using Kalign (EMBL-EBI). Real-time PCR analysis was performed using the following primers: *Alt* (F-aactagctgtcccgtctcca and R–ctctgatgagccactgcaag), *Otc* (F- acctgggct cagttagggtag R-cgtcatgatttgtaatgacctaaga), 28S (F- ctgggtataggggcgaaagac R- ggccccaagacctctaatcat), nontarget region (F- cctctgtgcctgtgaagga R- catcagtgtcccctgacaga). The relative abundance was normalized to abundance of 28S between the input and immunoprecipitated samples as previously described (Tuteja et al., 2009).

Neurobehavioral Analysis

See Supplemental Information.

Human Study

We studied 10 adult participants [5 female; mean age 25.5 years (range 19–41 years); mean body mass index 25.1 kg/m2 (20–28 kg/m2)], as previously

http://doc.rero.ch

published (Scheer et al., 2009). The forced desynchrony protocol consisted of 7 recurring 28-hr sleep/wake cycles under dim light conditions (±1.8 lux) to minimize any influence of light on the circadian system. During this period a fasting plasma sample was collected from each participant every 28 hr across the full 196 hr of the forced desynchrony, with each sample collected approximately 12 hr after the last meal (within 1 hr of awakening and prior to breakfast). By analyzing the plasma samples every 28 hr throughout the forced desynchrony protocol, samples were distributed across the circadian cycle, allowing assessment of the effects of the circadian system, independent of the effects of the behavioral cycles of sleep/fasting and wake/eating (Scheer et al., 2009). A sufficient number of samples across the entire circadian cycle was available for analysis in 8 of these 10 participants.

Statistical Analysis

All data are presented as mean ± SEM. For circadian mouse studies, the statistical significance between time points to assess rhythmicity was performed using analysis of variance (ANOVA). The statistical difference between two individual groups was assessed using the Student's t test; $p < 0.05$ was considered significant. For the human forced desynchrony protocol, the effect of the endogenous circadian rhythm was analyzed using cosinor analyses, including the circadian (fundamental ~24-hr) rhythmicity and a linear component (hours since the start of the forced desynchrony protocol) and mixed model analysis of variance with restricted maximum likelihood (REML) estimates of the variance components (JMP, SAS Institute) (Nelson et al., 1979). For analytes without significant effect of the linear component, a simple cosine model was used. Continuously recorded core body temperature was used as individualized circadian phase marker in the human study (Scheer et al., 2009).

SUPPLEMENTAL INFORMATION

Supplemental Information includes Supplemental Experimental Procedures, seven figures, and one table and can be found with this article online at doi:10.1016/j.cmet.2012.01.020.

ACKNOWLEDGMENTS

We are grateful to Drs. Alfred F. Connors, Jr., David S. Rosenbaum, Jonathan S. Stamler, Douglas T. Hess, and Satish C. Kalhan for support and suggestions, to Dr. Ueli Schibler for reagents, to Drs. John Le Lay and Klaus H. Kaestner for providing chromatin immunoprecipitation protocol, to Ken Grimes and Wanda Snead at the Vanderbilt MMPC, to Dana Lee at the Cincinnati MMPC, to Jenny Marks at BWH, to Diana Awad Scrocco for proofreading, to Mike Mustar for artistic illustrations, to the CWRU Rodent Behavior Core, and to members of the Jain laboratory for their assistance. Funding sources: NIH grants HL094660 (D.J.), R01-HL09480601 and P30-HL101299 (F.A.J.L.S.); K24-HL76446 (S.A.S.); HL072952 (S.M.H.); HL097023 (G.H.M.); HL075427, HL076754, HL084154, HL086548, and HL097595 (M.K.J.); DK059630 (Cincinnati MMPC); DK59637 (Vanderbilt MMPC); SNF grant 31003A/131086 (U.A.); and M01-RR02635 (BWH).

Received: April 8, 2011
Revised: October 10, 2011
Accepted: January 27, 2012
Published online: March 6, 2012

REFERENCES

Balandreau, J.P., Millier, C.R., and Dommergues, Y.R. (1974). Diurnal variations of nitrogenase activity in the field. Appl. Microbiol. *27*, 662–665.

Bauer, A., Urquhart, A.A., and Joy, K.W. (1977). Amino Acid metabolism of pea leaves: diurnal changes and amino Acid synthesis from N-nitrate. Plant Physiol. *59*, 915–919.

Brosnan, M.E., and Brosnan, J.T. (2009). Hepatic glutamate metabolism: a tale of 2 hepatocytes. Am. J. Clin. Nutr. *90*, 857S–861S.

D'Antona, G., Ragni, M., Cardile, A., Tedesco, L., Dossena, M., Bruttini, F., Caliaro, F., Corsetti, G., Bottinelli, R., Carruba, M.O., et al. (2010). Branched-chain amino acid supplementation promotes survival and supports cardiac and skeletal muscle mitochondrial biogenesis in middle-aged mice. Cell Metab. *12*, 362–372.

Damiola, F., Le Minh, N., Preitner, N., Kornmann, B., Fleury-Olela, F., and Schibler, U. (2000). Restricted feeding uncouples circadian oscillators in peripheral tissues from the central pacemaker in the suprachiasmatic nucleus. Genes Dev. *14*, 2950–2961.

Dibner, C., Schibler, U., and Albrecht, U. (2010). The mammalian circadian timing system: organization and coordination of central and peripheral clocks. Annu. Rev. Physiol. *72*, 517–549.

Duez, H., and Staels, B. (2008). The nuclear receptors Rev-erbs and RORs integrate circadian rhythms and metabolism. Diab. Vasc. Dis. Res. *5*, 82–88.

Feigin, R.D., Klainer, A.S., and Beisel, W.R. (1967). Circadian periodicity of bloof amino-acids in adult men. Nature *215*, 512–514.

Feigin, R.D., Dangerfield, H.G., and Beisel, W.R. (1969). Circadian periodicity of blood amino acids in normal and adrenalectomized mice. Nature *221*, 94–95.

Felig, P. (1975). Amino acid metabolism in man. Annu. Rev. Biochem. *44*, 933–955.

Fernstrom, J.D., Wurtman, R.J., Hammarstrom-Wiklund, B., Rand, W.M., Munro, H.N., and Davidson, C.S. (1979). Diurnal variations in plasma neutral amino acid concentrations among patients with cirrhosis: effect of dietary protein. Am. J. Clin. Nutr. *32*, 1923–1933.

Fisch, S., Gray, S., Heymans, S., Haldar, S.M., Wang, B., Pfister, O., Cui, L., Kumar, A., Lin, Z., Sen-Banerjee, S., et al. (2007). Kruppel-like factor 15 is a regulator of cardiomyocyte hypertrophy. Proc. Natl. Acad. Sci. USA *104*, 7074–7079.

Foster, R.G., and Roenneberg, T. (2008). Human responses to the geophysical daily, annual and lunar cycles. Curr. Biol. *18*, R784–R794.

Grandison, R.C., Piper, M.D., and Partridge, L. (2009). Amino-acid imbalance explains extension of lifespan by dietary restriction in Drosophila. Nature *462*, 1061–1064.

Gray, S., Wang, B., Orihuela, Y., Hong, E.G., Fisch, S., Haldar, S., Cline, G.W., Kim, J.K., Peroni, O.D., Kahn, B.B., and Jain, M.K. (2007). Regulation of gluconeogenesis by Krüppel-like factor 15. Cell Metab. *5*, 305–312.

Green, C.B., Takahashi, J.S., and Bass, J. (2008). The meter of metabolism. Cell *134*, 728–742.

Gropman, A.L., Summar, M., and Leonard, J.V. (2007). Neurological implications of urea cycle disorders. J. Inherit. Metab. Dis. *30*, 865–879.

Haldar, S.M., Lu, Y., Jeyaraj, D., Kawanami, D., Cui, Y., Eapen, S.J., Hao, C., Li, Y., Doughman, Y.Q., Watanabe, M., et al. (2010). Klf15 deficiency is a molecular link between heart failure and aortic aneurysm formation. Sci. Transl. Med. *2*. 10.1126/scitranslmed.3000502.

Harper, A.E., Miller, R.H., and Block, K.P. (1984). Branched-chain amino acid metabolism. Annu. Rev. Nutr. *4*, 409–454.

Hogenesch, J.B., Gu, Y.Z., Moran, S.M., Shimomura, K., Radcliffe, L.A., Takahashi, J.S., and Bradfield, C.A. (2000). The basic helix-loop-helix-PAS protein MOP9 is a brain-specific heterodimeric partner of circadian and hypoxia factors. J. Neurosci. *20*, RC83.

Ko, C.H., and Takahashi, J.S. (2006). Molecular components of the mammalian circadian clock. Hum. Mol. Genet. *15* (Spec No 2), R271–R277.

Lamia, K.A., Storch, K.F., and Weitz, C.J. (2008). Physiological significance of a peripheral tissue circadian clock. Proc. Natl. Acad. Sci. USA *105*, 15172–15177.

Le Martelot, G., Claudel, T., Gatfield, D., Schaad, O., Kornmann, B., Sasso, G.L., Moschetta, A., and Schibler, U. (2009). REV-ERBalpha participates in circadian SREBP signaling and bile acid homeostasis. PLoS Biol. *7*, e1000181.

Lee, J.T., and Nussbaum, R.L. (1989). An arginine to glutamine mutation in residue 109 of human ornithine transcarbamylase completely abolishes enzymatic activity in Cos1 cells. J. Clin. Invest. *84*, 1762–1766.

Marcheva, B., Ramsey, K.M., Buhr, E.D., Kobayashi, Y., Su, H., Ko, C.H., Ivanova, G., Omura, C., Mo, S., Vitaterna, M.H., et al. (2010). Disruption of the clock components CLOCK and BMAL1 leads to hypoinsulinaemia and diabetes. Nature *466*, 627–631.

http://doc.rero.ch

McConnell, B.B., and Yang, V.W. (2010). Mammalian Krüppel-like factors in health and diseases. Physiol. Rev. *90*, 1337–1381.

Miller, I.J., and Bieker, J.J. (1993). A novel, erythroid cell-specific murine transcription factor that binds to the CACCC element and is related to the Krüppel family of nuclear proteins. Mol. Cell. Biol. *13*, 2776–2786.

Minami, Y., Kasukawa, T., Kakazu, Y., Iigo, M., Sugimoto, M., Ikeda, S., Yasui, A., van der Horst, G.T., Soga, T., and Ueda, H.R. (2009). Measurement of internal body time by blood metabolomics. Proc. Natl. Acad. Sci. USA *106*, 9890–9895.

Morris, S.M., Jr. (2002). Regulation of enzymes of the urea cycle and arginine metabolism. Annu. Rev. Nutr. *22*, 87–105.

Nelson, W., Tong, Y.L., Lee, J.K., and Halberg, F. (1979). Methods for cosinor-rhythmometry. Chronobiologia *6*, 305–323.

Newgard, C.B., An, J., Bain, J.R., Muehlbauer, M.J., Stevens, R.D., Lien, L.F., Haqq, A.M., Shah, S.H., Arlotto, M., Slentz, C.A., et al. (2009). A branched-chain amino acid-related metabolic signature that differentiates obese and lean humans and contributes to insulin resistance. Cell Metab. *9*, 311–326.

Oster, H., Yasui, A., van der Horst, G.T., and Albrecht, U. (2002). Disruption of mCry2 restores circadian rhythmicity in mPer2 mutant mice. Genes Dev. *16*, 2633–2638.

Preitner, N., Damiola, F., Lopez-Molina, L., Zakany, J., Duboule, D., Albrecht, U., and Schibler, U. (2002). The orphan nuclear receptor REV-ERBalpha controls circadian transcription within the positive limb of the mammalian circadian oscillator. Cell *110*, 251–260.

Reddy, A.B., Karp, N.A., Maywood, E.S., Sage, E.A., Deery, M., O'Neill, J.S., Wong, G.K., Chesham, J., Odell, M., Lilley, K.S., et al. (2006). Circadian orchestration of the hepatic proteome. Curr. Biol. *16*, 1107–1115.

Reppert, S.M., and Weaver, D.R. (2002). Coordination of circadian timing in mammals. Nature *418*, 935–941.

Rey, G., Cesbron, F., Rougemont, J., Reinke, H., Brunner, M., and Naef, F. (2011). Genome-wide and phase-specific DNA-binding rhythms of BMAL1 control circadian output functions in mouse liver. PLoS Biol. *9*, e1000595.

Ripperger, J.A., and Schibler, U. (2006). Rhythmic CLOCK-BMAL1 binding to multiple E-box motifs drives circadian Dbp transcription and chromatin transitions. Nat. Genet. *38*, 369–374.

Rudic, R.D., McNamara, P., Curtis, A.M., Boston, R.C., Panda, S., Hogenesch, J.B., and Fitzgerald, G.A. (2004). BMAL1 and CLOCK, two essential components of the circadian clock, are involved in glucose homeostasis. PLoS Biol. *2*, e377.

Scheer, F.A., Hilton, M.F., Mantzoros, C.S., and Shea, S.A. (2009). Adverse metabolic and cardiovascular consequences of circadian misalignment. Proc. Natl. Acad. Sci. USA *106*, 4453–4458.

Shah, S.H., Bain, J.R., Muehlbauer, M.J., Stevens, R.D., Crosslin, D.R., Haynes, C., Dungan, J., Newby, L.K., Hauser, E.R., Ginsburg, G.S., et al. (2010). Association of a peripheral blood metabolic profile with coronary artery disease and risk of subsequent cardiovascular events. Circ Cardiovasc Genet *3*, 207–214.

Shi, S., Hida, A., McGuinness, O.P., Wasserman, D.H., Yamazaki, S., and Johnson, C.H. (2010). Circadian clock gene Bmal1 is not essential; functional replacement with its paralog, Bmal2. Curr. Biol. *20*, 316–321.

Tu, B.P., Mohler, R.E., Liu, J.C., Dombek, K.M., Young, E.T., Synovec, R.E., and McKnight, S.L. (2007). Cyclic changes in metabolic state during the life of a yeast cell. Proc. Natl. Acad. Sci. USA *104*, 16886–16891.

Turek, F.W., Joshu, C., Kohsaka, A., Lin, E., Ivanova, G., McDearmon, E., Laposky, A., Losee-Olson, S., Easton, A., Jensen, D.R., et al. (2005). Obesity and metabolic syndrome in circadian Clock mutant mice. Science *308*, 1043–1045.

Tuteja, G., White, P., Schug, J., and Kaestner, K.H. (2009). Extracting transcription factor targets from ChIP-Seq data. Nucleic Acids Res. *37*, e113.

Vollmers, C., Gill, S., DiTacchio, L., Pulivarthy, S.R., Le, H.D., and Panda, S. (2009). Time of feeding and the intrinsic circadian clock drive rhythms in hepatic gene expression. Proc. Natl. Acad. Sci. USA *106*, 21453–21458.

Wang, J., Alexander, P., Wu, L., Hammer, R., Cleaver, O., and McKnight, S.L. (2009). Dependence of mouse embryonic stem cells on threonine catabolism. Science *325*, 435–439.

Wheeler, C.T. (1969). Diurnal Fluctuation in Nitrogen Fixation in Nodules of Alnus Glutinosa and Myrica Gale. New Phytol. *68*, 675.

Wu, G. (2009). Amino acids: metabolism, functions, and nutrition. Amino Acids *37*, 1–17.

Ye, X., Robinson, M.B., Batshaw, M.L., Furth, E.E., Smith, I., and Wilson, J.M. (1996). Prolonged metabolic correction in adult ornithine transcarbamylase-deficient mice with adenoviral vectors. J. Biol. Chem. *271*, 3639–3646.

Yin, L., Wu, N., Curtin, J.C., Qatanani, M., Szwergold, N.R., Reid, R.A., Waitt, G.M., Parks, D.J., Pearce, K.H., Wisely, G.B., et al. (2007). Rev-erbalpha, a heme sensor that coordinates metabolic and circadian pathways. Science *318*, 1786–1789.

Zheng, B., Albrecht, U., Kaasik, K., Sage, M., Lu, W., Vaishnav, S., Li, Q., Sun, Z.S., Eichele, G., Bradley, A., et al. (2001). Nonredundant roles of the mPer1 and mPer2 genes in the mammalian circadian clock. Cell *105*, 683–694.

http://doc.rero.ch